A Traveling-wave Tube Coupled with Directional Coupler

Yoshihiko OGAWA

Contents

Abstract 357
I. Introduction 357
II. The Directional Coupler 359
III. Amplification 360
IV. Small ε or Weak Coupling Directional Coupler 363
V. Large ε or Strong Coupling Directional Coupler 366
VI. The Rigorous Analysis not Neglecting the Fast Electron Space-Charge Wave 371
VII. Conclusion 373
Acknowledgment 373
References 373

Abstract

The high efficiency of a traveling-wave tube is required in some practical fields at present. The present paper deals with the advancing of a theory concerning a new type of tube. A comparison of tubes with weak copuling strength at the coupled wall, as against that with strong coupling strength lead to some interesting aspects.

I. Introduction

One of the largest defects of a conventional traveling-wave tube comes from the use of graphite coating, or aquadag in order to attenuate the reflex wave which is caused by the imperfect matching between a helix and external circuits at the points of input and output. The main reasons for this are: (1) the forward wave is simultaneously attenuated by this coating, making the helix length undesirably long, (2) the large-signal operation is considerably restricted by the r–f loss produced in the attenuator in which this restriction is one of the reasons that the efficiency of the conventional traveling-wave tube becomes very bad. If the problem in mismatching at the points of input and output can be solved, one should expect to remove the graphite coating from the traveling-wave tube.

Instead of the concentric coupling which has been used in conventional traveling-wave tubes, the use of the distributed coupling between the external

circuit and the traveling-wave tube may be one of the means for removing the coating. The deviced coupling unit is shown schematically in Fig. 1. The slow-wave circuit structures (1) and (2) are mutually coupled by the coupled wall, and an electron beam passes through the slow-wave structure (2). The input wave comes from the left-hand side of the slow-wave structure (1) and the amplified output wave comes out of the right-hand side of the structure (1). Another output wave comes out of the right-hand side of the structure (2), but this wave must be perfectly attenuated with the attenuator at this point. The reflex wave, if any, may be excluded by the attenuator at the left-hand side of the structure (2). When the coupling strength of the coupled wall is gradually varied near the points of input and output in order to get good matching, this type of amplifier described above may not need any attenuator in the interaction region as the conventional amplifier requires.

The results obtained from the power gain calculations for this amplifier show the following interesting facts, depending on the coupling strength:

(1) weak coupling strength

In this case, the reflex wave can be easily suppressed. Moreover at some proper coupling strength, this new type of tube produces the exponential power gain due to the wider range of the electron beam velocity than the conventional tube. This fact and that of requiring no graphite coating in the interaction region may be the desirable reasons for the large-signal operation.

(2) strong coupling strength

In this case, the range of the electron beam velocity producing the exponential power gain is divided into two parts; i.e. one is the range of the faster velocity and the other is the slower when compared with the velocity of the conventional tube. In the latter case, the dimensions of the slow-wave structure may be changeable toward the larger scale without slowing the electron velocity.

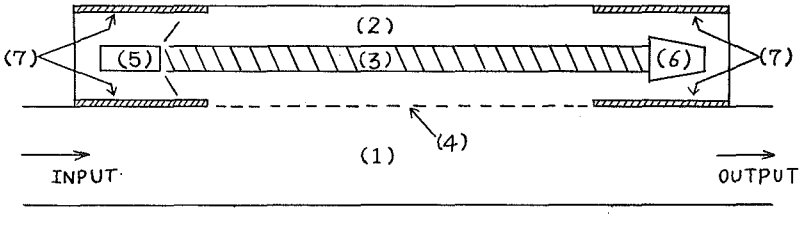

Fig. 1. Schetch of traveling-wave tube coupled with directional coupler; (1) slow-wave circuit structure (I); (2) slow-wave circuit structure (II); (3) electron beam; (4) coupled wall; (5) electron gun; (6) collector; (7) attenuators.

II. The Directional Coupler[1]

In Fig. 1, supposing that the electron beam is excluded and considering that the only two remaining circuits are coupled with the coupled wall, the coupling equations for these cricuits can be written as follows

$$\left.\begin{aligned}(d/dz+j\beta_1)a_1 &= C_{12}a_2\\ (d/dz+j\beta_2)a_2 &= C_{21}a_1\end{aligned}\right\} \qquad (1)$$

where β_1 and β_2 are the longitudinal, or z-directional propagation constants of the slow-wave circuits (1) and (2) respectively, in the case of the absence of coupling. C_{12} and C_{21} are the mutual coupling coefficients per unit length. The mode, or wave amplitudes $a_i(i=1, 2)$, where a_1 is the mode amplitude of the circuit wave (1) and a_2 is that of the circuit wave (2), are normalized so that $2|a_i(i=1, 2)|$ represents the average power carried by each mode.

Since the circuits (1) and (2) are coupled passively, the next relationship exists between C_{12} and C_{21}

$$C_{12} = -C_{21}^* \qquad (2)$$

Generally C_{12} and C_{21} are complex numbers, but when the circuits are lossless these values are pure imaginary. (We assume only lossless circuits hereafter.)

Solutions of the coupled mode equations (1), are of the form $\exp(-j\beta z)$. When this form is substituted in the Eqs. (1), the next equation on the eigen-value β can be introduced

$$(\beta-\beta_1)(\beta-\beta_2)-|C_{12}|^2 = 0 \qquad (3)$$

Now put

$$\beta_1 \equiv \beta_c(1+\Delta), \quad \beta_2 \equiv \beta_c \qquad (4)$$

Then from Eq. (3), the roots of β are easily found to be β_t and β_l, where

$$\beta_{t,l} = \beta_c(1+\Delta/2) \pm \sqrt{(\Delta/2)^2+|C_{12}|^2} \qquad (5)$$

(the upper sign shows β_t and the lower β_l.)

Now assume that the radial propagation constants are $\gamma_{t,l}$, then

$$\gamma_{t,l} = \sqrt{\beta_{t,l}^2-\beta_0^2} \qquad (6)$$

where β_0 is the free space propagation constant and it can be neglected so that the approximation of Eq. (6) become as follows

$$\gamma_{t,l} \fallingdotseq \beta_{t,l} \qquad (7)$$

The $\gamma_{t,l}$ can be solved from the field equations. When β_c, Δ and $\gamma_{t,l}$ are known, the absolute value of the mutual coupling coefficient per unit length $|C_{12}|$ are

$$|C_{12}| = \sqrt{\{(\gamma_f - \gamma_l)/2\}^2 - (\Delta/2)^2} \tag{8}$$

The next step is to study the r-f power to be carried by both circuits (1) and (2). If all the power is put on the circuit (1) at $z=0$ initially, then $a_2(z=0)=0$ and $a_1(z=0)=1/2$, and the power carried by each circuit is found to be

$$\left.\begin{aligned} P_1(z) &= 2|a_1(z)|^2 = 1 - F\sin^2\sqrt{(\Delta/2)^2+|C_{12}|^2}\,z \\ P_2(z) &= 2|a_2(z)|^2 = 1 - P_1(z) = F\sin\sqrt{(\Delta/2)^2+|C_{12}|^2}\,z \end{aligned}\right\} \tag{9}$$

where,

$$F = 1\Big/\left\{1+(\beta_e\Delta/2|C_{12}|)^2\right\} \tag{10}$$

F is called as the transfer factor between the circuits (1) and (2). By Eq. (9) and (10) it is seen that complete power transfer takes place, if $\Delta=0$ (synchronous case), in a length L as given by

$$L = (2n-1)/2|C_{12}|, \qquad n = 1, 2, 3, \cdots \tag{11}$$

but it is incomplete if $\Delta \neq 0$ (nonsynchronous case).

The above discussion can be applied actually for the reflex wave from the output end of the circuit (1) shown in Fig. 1, because the electron beam can not interact with the reflex wave at all. So if the circuit length is selected to satisfy Eq. (11), the maximum power is supplied to the left-hand side of the circuit (2) and attenuated completely by the attenuator. In this case it is desirable that Δ is as small as possible (the best case is $\Delta=0$). But if Δ is not small enough under any inevitable condition such as the use of coupled helices etc., the power remains in the input end of the circuit (1), and we must insert the isolator there when this remaining power is undesirable.

III. Amplification

It is, for simplicity, assumed that there is no coupling between the circuit (1) and the electron beam, and that the fast electron space-charge wave can not be coupled to both circuit waves (1) and (2). Then the coupling equations are[2)]

$$\left.\begin{aligned} \left\{d/dz + j\beta_e(1+\Delta)\right\} a_1 &= C_{12}a_2 \\ (d/dz + j\beta_e)\,a_2 &= C_{21}a_1 + C_{23}a_3 \\ \left\{d/dz + j(\beta_e+\beta_q)\right\} a_3 &= C_{32}a_2 \end{aligned}\right\} \tag{12}$$

where, a_1, a_2 and a_3 are the normalized mode amplitudes of the circuit wave (1), the circuit wave (2) and the slow electron space-charge wave respectively.

The relationship between C_{12} and C_{21} is shown in Eq. (2), and the relationship between C_{23} and C_{32}, which are the active coupling coefficients, can be written as follows

$$C_{23} = C_{32}^* \tag{13}$$

Similar to the case of C_{12} and C_{21}, C_{23} and C_{32} are also generally complex numbers, but these are the pure imaginary when the circuits are lossless.

Solutions of the coupled mode equations (12) are of the form $\exp(-\Gamma' z)$. If Γ, β_e and β_q are rewritten by Pierce's parameters, C, QC and b (gain parameter, space-charge parameter and velocity parameter, respectively), then

$$\left.\begin{aligned} \Gamma &= j\beta_e(1+jC\delta) \\ \beta_e &= \beta_e(1+Cb) \\ \beta_q &= \beta_e C\sqrt{4QC} \end{aligned}\right\} \tag{14}$$

where, $\beta_e = \omega/v_0$ and v_0 is the d.c. electron velocity.

Substituting Eq. (14) into Eq. (12), the next determinantal equation must be satisfied if Eq. (12) possess non-trivial solutions:

$$\begin{vmatrix} j\beta_e C\{b-j\delta+(1+Cb)\Delta/C\} & -C_{12} & 0 \\ -C_{12} & j\beta_e C(b-j\delta) & -C_{23} \\ 0 & C_{23} & j\beta_e C(\sqrt{4QC}-j\delta) \end{vmatrix} = 0 \tag{15}$$

Eq. (15) can be rewritten as follows

$$\eta^3 + f\eta + g = 0 \tag{16}$$

where,

$$\left.\begin{aligned} f &= 1-\varepsilon^2+\nu\lambda-(\nu+\lambda)^2/3 \\ g &= (2/27)(\nu+\lambda)^3-(1/3)(\nu+\lambda)(1-\varepsilon^2+\nu\lambda)+\lambda-\nu\varepsilon^2 \end{aligned}\right\} \tag{17}$$

and

$$\left.\begin{aligned} \eta &= \left[4b/3-\{\sqrt{4QC}+(1+Cb)\Delta/C\}/3-j\delta\right]/C \\ |C_{23}'| &= |C_{23}|/\beta_e C = j/\sqrt{2}\,(4QC)^{1/4} \\ \varepsilon &= |C_{12}/C_{23}| \\ \nu &= (\sqrt{4QC}-b)/|C_{23}'| \\ \lambda &= (1+Cb)\Delta/C|C_{23}'| \end{aligned}\right\} \tag{18}$$

Strictly speaking, both ε and λ are functions of ν such that

$$\left.\begin{aligned}
&\varepsilon = \varepsilon_0(1-s\nu)\\
&\lambda = \lambda_0(1-s\nu)\\
&\varepsilon_0 = (1/\sqrt{2}\sqrt[4]{4QC})(|C_{12}|/\beta_o)(1+C\sqrt{4QC})/C\\
&\lambda_0 = \sqrt{2}\sqrt[4]{4QC}\,\Delta(1+C\sqrt{4QC})/C\\
&s = C/\sqrt{2}\sqrt[4]{4QC}(1+C\sqrt{4QC})
\end{aligned}\right\} \tag{19}$$

By using Eq. (19), Eq. (17) can be rewritten as follows

$$\left.\begin{aligned}
f = &-(1/3)\left\{1+\lambda_0 s+(\lambda_0 s)^2+3(\varepsilon_0 s)^2\right\}\nu^2+(1/3)(\lambda_0+2\lambda_0^2 s\\
&+6\varepsilon_0^2 s)\nu+1-\varepsilon_0^2-\lambda_0^2/3\\
g = &\,(1/27)\left\{2+3\lambda_0 s-3(\lambda_0 s)^2-2(\lambda_0 s)^3-9(\lambda_0 s)(\varepsilon_0 s)^2\right.\\
&\left.-18(\varepsilon_0 s)^2\right\}\nu^3+(1/27)\left\{-3\lambda_0+6\lambda_0^2 s+6\lambda_0^3 s^2+27\lambda_0\varepsilon_0^2 s^2\right.\\
&\left.+36\varepsilon_0^2 s\right\}\nu^2-(1/27)\left\{9+3\lambda_0^2+18\lambda_0 s+6\lambda_0^3 s+27\lambda_0\varepsilon_0^2 s\right.\\
&\left.+18\varepsilon_0^2\right\}\nu+(\lambda_0/27)(18+2\lambda_0^2+9\varepsilon_0^2)
\end{aligned}\right\} \tag{20}$$

Generally $0<s\ll 1$ so that, if the each magnitude of ε_0, λ_0 and ν are as large as one, then instead of using Eq. (20) we can use Eq. (17) by considering $\varepsilon \fallingdotseq \varepsilon_0$ and $\lambda \fallingdotseq \lambda_0$.

Now suppose that the roots of η in Eq. (16) are η_1, η_2 and η_3 respectively, then

$$\left.\begin{aligned}
&\eta_1 = u+v\\
&\eta_2 = -(u+v)/2+j(\sqrt{3}/2)(u-v)\\
&\eta_3 = \eta_2^* = -(u+v)-j(\sqrt{3}/2)(u-v)
\end{aligned}\right\} \tag{21}$$

or representing η_i by δ_i $(i=1, 2, 3)$

$$\left.\begin{aligned}
&\delta_1 = j\left[(u+v)|C_{23}'|-4b/3+\left\{\sqrt{4QC}+(1+Cb)\Delta/C\right\}/3\right]\\
&\delta_2 = -\delta_1/2-(\sqrt{3}/2)(u-v)|C_{23}'|\\
&\delta_3 = -\delta_1/2+(\sqrt{3}/2)(u-v)|C_{23}'|
\end{aligned}\right\} \tag{21'}$$

where

$$\left.\begin{aligned}
&u = (-g/2+\sqrt{R})^{1/3}\\
&v = (-g/2-\sqrt{R})^{1/3}\\
&R = g^2/4+f^3/27
\end{aligned}\right\} \tag{22}$$

If $R>0$, then η_2 and η_3 (or δ_2 and δ_3) are the complex roots, and in this case the exponentially growing wave should exist.

IV. Small ε or Weak Coupling Directional Coupler

In Fig. 2 the solutions of $|\mathrm{Real}(\delta/|C_{23}'|)|$ are shown when Δ (or λ)$=0$ and ε and ν are as large as one.

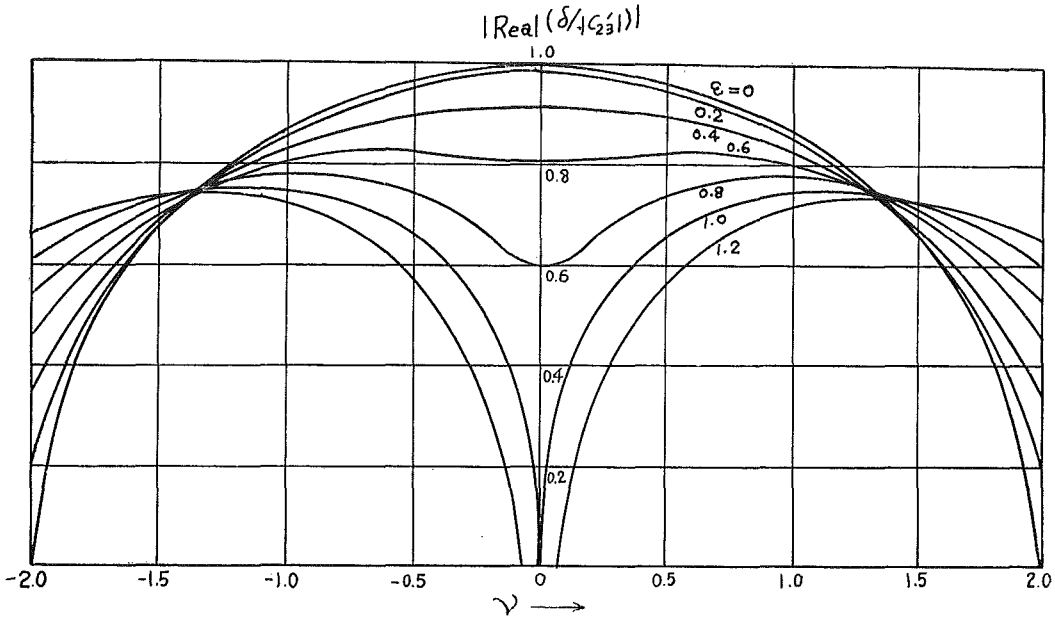

Fig. 2. $|\mathrm{Real}(\delta/|C_{23}'|)|$ versus ν for $\lambda=0$

The coupling strength for $\varepsilon\sim1$, is very weak. For example, in the case of $(1+Cb)/\sqrt{2}\sqrt[4]{4QC}\sim1$ and $\varepsilon\sim1$, it becomes to be $|C_{12}|\sim\beta_e C$ by Eq. 19, and usually $C\ll1$ exists to be $|C_{12}|\ll\beta_e$.

It can be seen from Fig. 2 that, although the maximum gain for $0.6<\varepsilon<0.8$ is somewhat smaller than that for $\varepsilon=0$ (the conventional traveling-wave tube case), the range of ν (or the electron beam velocity range) producing the exponentially growing wave is significantly wider for the former than the latter. This result leads the following consideration. With the reference of Eq. (5), the two propagation constants β_t and β_l being different from each other (the former is smaller than the latter) are in existence in the directional coupler of this kind, and the power transfer shown by Eq. (9) is due to the beat action of the two waves having different phase velocities. Now the electron beam can interact with both β_t- and β_l-waves, but it must move faster whenever synchronizing with the former wave, than the latter. As shown by the dashed curves in Fig. 3, therefore, the two gain curves produced by interactions with β_t- and

β_t-waves, are separated from each other, and the resulting gain curve becomes as indicated by the solid curve in Fig. 3. The tendency of the separation increases with increase in ε (or the mutual coupling coefficient $|C_{12}|$). This tendency is shown by the arrow marks until the perfect separation occurs, where the curve is shown by the broken curve in Fig. 3.

Because of the above mentioned reasons, the range of ν producing the growing wave should be wider in some values of ε (or $|C_{12}|$) before the occurance of the perfect separation than in the value at $\varepsilon=0$ which is the case of the conventional traveling-wave tube.

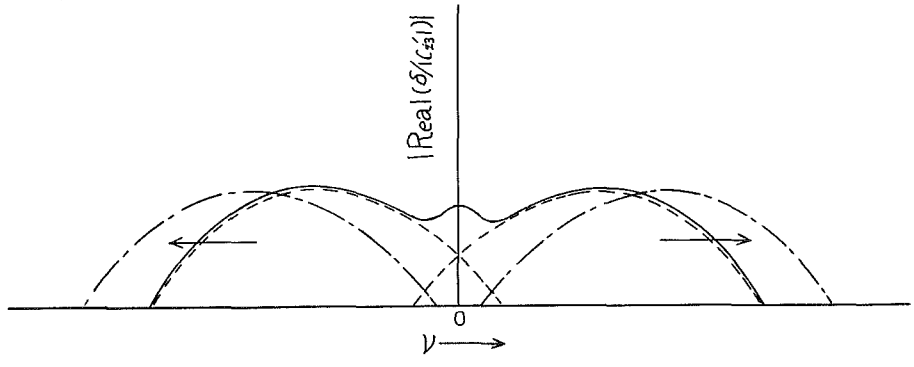

Fig. 3. Illustration of the results of Fig. 2

It must be the necessary condition for the improvement of the efficiency in the large-signal operation of the traveling-wave tube that the exponentially growing wave occurs in wide range of the electron beam velocity, so that the condition of $0.6<\varepsilon<0.8$ is desirable for the large-signal operation. Another advantage may rise in the case of the weak coupling by removing the reflex wave easily.

Next considering is the initial loss. From the results of Eq. (21′), $a_i(i=1, 2, 3)$ can be written as follows

$$\left.\begin{aligned} &a_i=\sum_{k=1}^{3} A_{ik}\exp(-\Gamma_k z), \qquad i=1, 2, 3\\ &\Gamma_k=j\beta_e(1+jC\delta_k)\end{aligned}\right\} \tag{23}$$

$A_{ik}(i, k=1, 2, 3)$ are determined by the initial conditions. Now for each $k(k=1, 2, 3)$, Eq. (13) must be satisfied so that

$$\left.\begin{aligned} &j\{b+(1+Cb)\Delta/C-j\delta_k\}A_{1k}-C_{12}'A_{2k}=0\\ &C_{23}'A_{2k}+j(\sqrt{4QC}-j\delta_k)A_{3k}=0\\ &k=1, 2, 3\end{aligned}\right\} \tag{24}$$

where

$$\left.\begin{aligned} &C_{12}' = C_{12}/\beta_e C \\ &A_{1k} = -\left\{|C_{12}'|/(\xi_k' - \lambda|C_{23}'|)\right\} A_{2k} \\ &A_{3k} = -\left\{|C_{23}'|/(\xi_k' + C_0)\right\} A_{2k} \\ &\xi_k' = b - j\delta_k \\ &C_0 = \sqrt{4QC} - b \end{aligned}\right\} \qquad (25)$$

The initial conditions are $a_1(z=0)=1$ and $a_2(z=0)=a_3(z=0)=0$ so that

$$\sum_{k=1}^{3} A_{ik} = \left\{\begin{array}{ll} 1, & i=1 \\ 0, & i=2,3 \end{array}\right\} \qquad (26)$$

From Eq. (25) and (26), referencing with Eq. (18), the following results can be obtained,

$$\left.\begin{aligned} &A_{1k} = \varepsilon H(\xi_k+\nu)(\xi_{k+1}-\xi_{k+2})/(\xi_k+\lambda) \\ &A_{2k} = H(\xi_k+\nu)(\xi_{k+1}-\xi_{k+2}) \\ &A_{3k} = -H(\xi_{k+1}-\xi_{k+2}) \\ &H = \left\{1/\varepsilon(\lambda-\nu)\right\} \prod_{k=1}^{3} (\xi_k+\lambda)/(\xi_k-\xi_{k+1}) \\ &k \equiv k+3, \qquad k=1,2,3 \end{aligned}\right\} \qquad (27)$$

where

$$\xi_k = \xi_k'/|C_{23}'|$$

If the circuit length is sufficiently long so as to be able to neglect the other non-growing two waves except the growing wave in Eq. (23), $a_1(z)$ can be written approximately as follows

$$a_1(z) \fallingdotseq \left\{\begin{array}{ll} A_{12}\exp(-\Gamma_2 z), & u-v<0 \\ A_{13}\exp(-\Gamma_3 z), & u-v>0 \end{array}\right\} \qquad (28)$$

It can be shown to be $A_{13}=A_{12}^*$ from Eq. (27). Instead of the form of $a_1(z)$, when required the gain representation G, G becomes

$$G = 20\log|a_1(z)| = 20\log|A| + 8.686\,\beta_e C|\mathrm{Real}\,(\delta)|\,z \quad db \qquad (29)$$

where

$$|A| \equiv |A_{12}| = |A_{13}|$$

In Eq. (29)the first term of the right-hand side represents the initial loss. The initial loss curves are shown in Fig. 4, when Δ (or λ)$=0$.

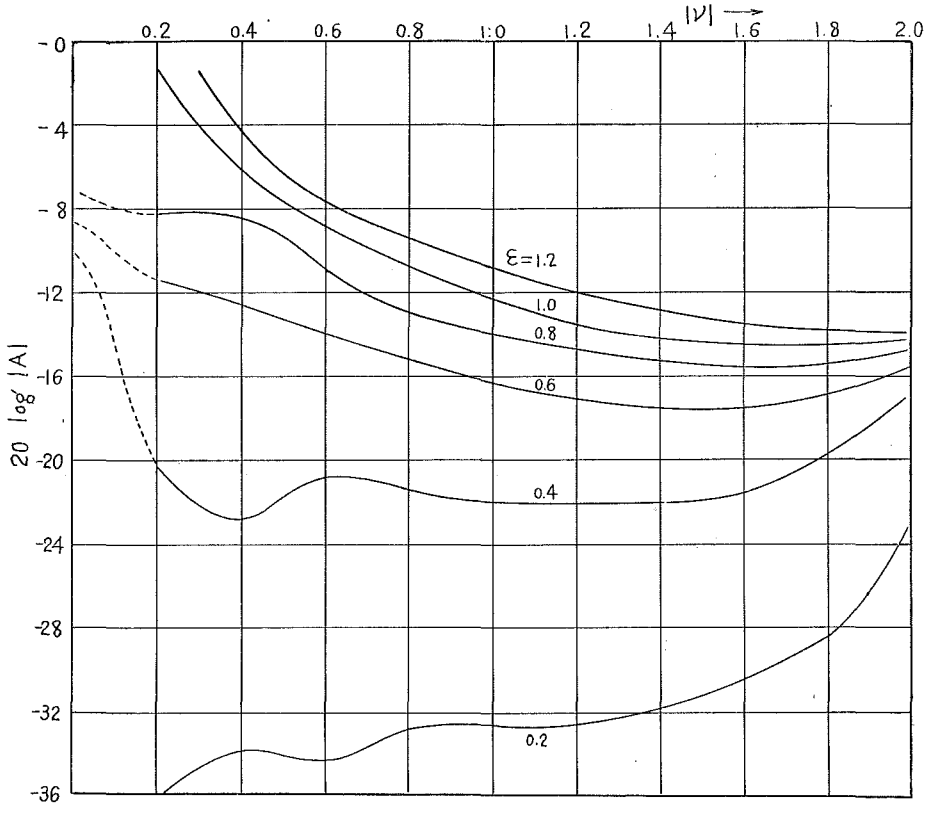

Fig. 4. Initial losses plotted as a function of ν for $\lambda=0$

(In Fig. 4 the oscillatory states in the small range of ν is due probably to the error introduced from the numerical calculations).

It must be remembered that the above discussion is true only in the large value of QC because the effect of the fast electron space-charge wave is neglected completely. In other words, the phase velocity of the wave must not be included in the region of the electron velocity producing the growing wave (if not so, the power absorption of the circuit wave occurs from the interaction with the fast electron space charge wave). This fact is also true in the case of large ε, i. e. in the case of the strong coupling.

If the effect of the fast wave is unavoidable, Eq. (12), the coupling equations, becomes useless.

V. Large ε or Strong coupling Directional Coupler

In this case we must take Eq. (20) in order to solve Eq. (21) instead of

Eq. (17), in which the calculation for solving Eq. (20) needs considerable elaboration when compared with the case of small ε. Because of the reason mentioned above, the calculation as an example was made for the one case among the cases of the coupled helices.

First the transverse propagation constant γ of one uncoupled helix can be solved from the field equations, or Maxwell's equations. It has been solved by Pierce as follows[3]

$$(\gamma a)^2 \frac{I_0(\gamma a) K_0(\gamma a)}{I_1(\gamma a) K_1(\gamma a)} = (\beta_0 a \cot \psi_1)^2 \tag{30}$$

where β_0 is the free-space propagation constant, a the helix radius, ψ_1 is the pitch angle and $I_\ell(x)$ and $K_\ell(x)$ the modified Bessel functions. Assuming that β is the longitudinal or z-directional propagation constant, β can be written as follows

$$\beta = \sqrt{\gamma^2 - \beta_0^2} \fallingdotseq \gamma \tag{31}$$

The relation of γa vs. $\beta_0 a \cot \psi_1$ is shown in Fig. 5.

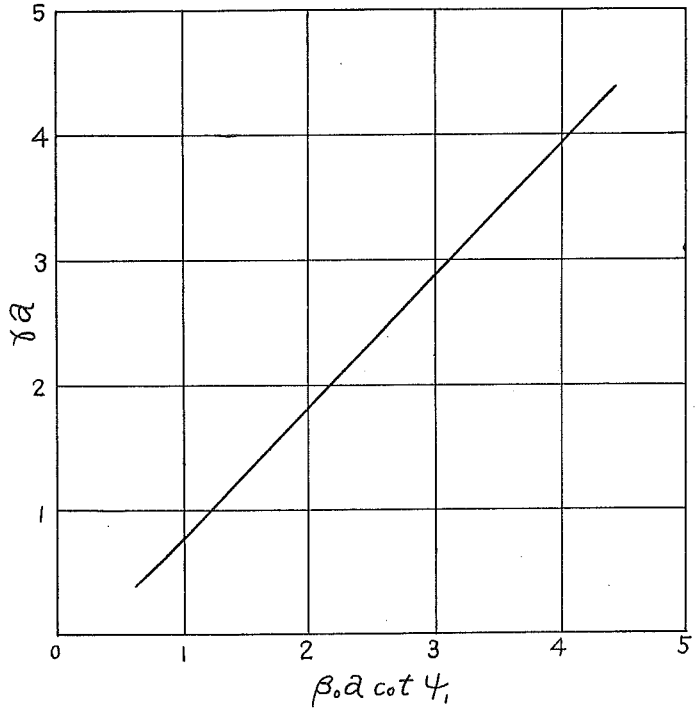

Fig. 5. The radial propagation constant plotted as a function of $\beta_0 a \cot \psi_1$

The next consideration is in the case of coupled helices. In Fig. 6, assuming that the radius and the pitch angle of inner helix are respectively a and ψ_1 and those of the outer helix respectively b and ψ_2, then the solution of the field equations is[4]

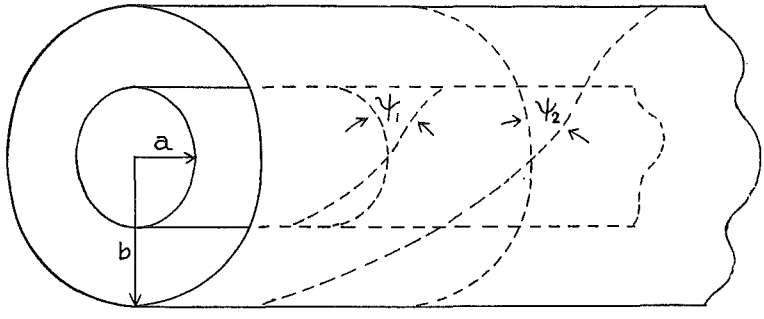

Fig. 6. Coupled helices arrangement

$$\left[R_0 - \frac{(\beta_0 a \cot\psi_1)^2}{(\gamma a)^2} \cdot \frac{\cot\psi_2}{\cot\psi_1} \cdot R_1\right] = \left[P_{02} - \frac{(\beta_0 a \cot\psi_1)^2}{(\gamma a)^2} \cdot P_{11}\right]\left[P_{02} - \frac{(\beta_0 a \cot\psi_2)^2}{(\gamma a)^2} \cdot P_{12}\right] \tag{32}$$

where

$$\left.\begin{aligned} P_{01} &\equiv I_0(\gamma a)K_0(\gamma a), \quad & P_{02} &\equiv I_0(\gamma b)K_0(\gamma b) \\ P_{11} &\equiv I_1(\gamma a)K_1(\gamma a), \quad & P_{12} &\equiv I_1(\gamma b)K_1(\gamma b) \\ R_0 &\equiv I_0(\gamma a)K_0(\gamma b), \quad & R_1 &\equiv I_1(\gamma a)K_1(\gamma b) \end{aligned}\right\} \tag{33}$$

From Eq. (32) the products of a and two roots of γ (i.e. γ_t and γ_l) can be solved as the functions of $\beta_0 a \cot\psi_1$. The values of γ_a and γ_b are assumed to be the transverse propagation constants of uncoupled inner and outer helices, respectively, and these values are obtained independently from Eq. (30). By using two roots of γ_t and γ_l and another two roots of γ_a and γ_b, $|C_{12}|$ can be obtained from Eq. (8) as a function of $\beta_0 a \cot\psi_1$, and $|C_{12}|$ is shown in Fig. 7 where the ratios of b/a and $\cot\psi_2/\cot\psi_1$ are 1.75 and -0.82, respectively (the minus sign of the latter shows to be wound mutually in opposite direction so as to get the strong coupling).

Introducing the following numerical example for the calculation of the exponential gain,

the frequency $f = 7760$ MC
$a = 1.25$ mm
$\cot\psi_1 = 8.355$

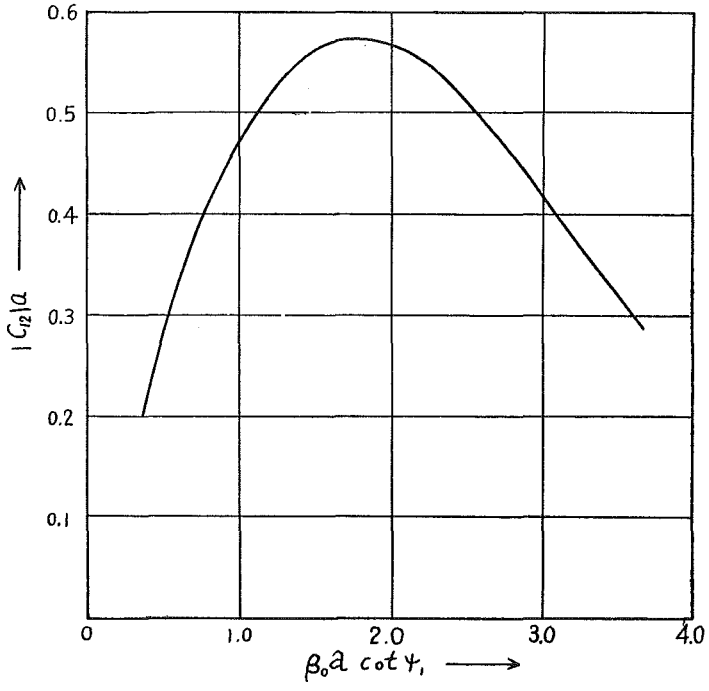

Fig. 7. The absolute value of the mutual coupling coefficient as a function of $\beta_0 a \cot \psi_1$ for $b/a=1.75$ and $\cot \psi_2/\cot \psi_1 = -0.82$

$$b/a = 1.75$$
$$\cot \psi_2/\cot \psi_1 = -0.82$$
$$C = 0.057$$
$$|C_{23}'| = 1/1.055$$
$$4QC = 0.31$$

(The values of C and $|C_{23}'|$ in the above equation correspond approximately to$I_0=35$ mA which is the mean electron beam current, and to $V_0=3000$ V which is the mean electron beam accelerating voltage.) In the above case, $|C_{12}|a$ is obtained from Fig. 7 as follows,

$$|C_{12}|a = 0.559 \tag{35}$$

By using Eq. (35) and Δ which can be easily obtained from γ_a and γ_b, the values of ε_0, λ_0 and s of Eq. (19) can be determined

$$\left.\begin{aligned} s &= 5.237\times 10^{-2} \\ \lambda_0 s &= -0.13 \\ \varepsilon_0 s &= 0.39 \end{aligned}\right\} \tag{36}$$

(It should be noted that β_e of Eq. (19) is the same as β_a.)

When substituting Eq. (36) into Eq. (20) and solving Eq. (21′) by using both newly calculated Eq. (20) and Eq. (22), the result of the relation between |Real (δ)| and ν can be introduced as shown in Fig. 8.

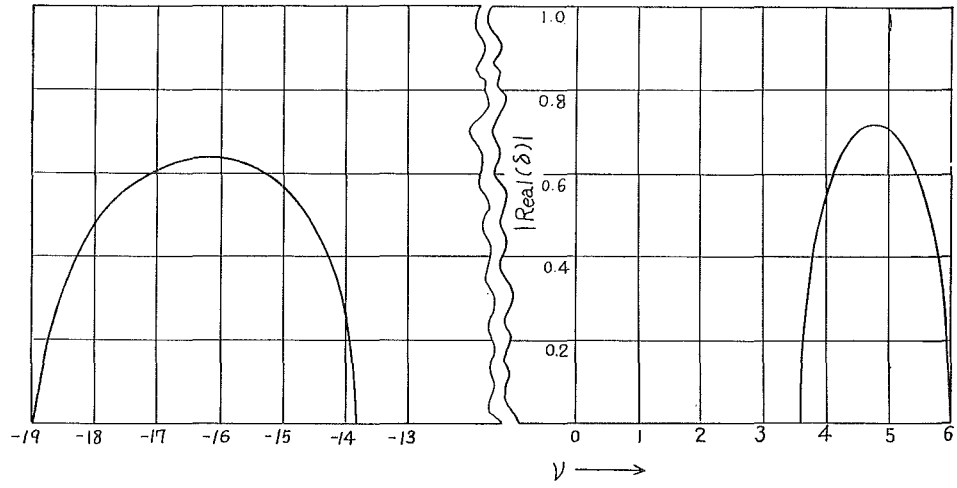

Fig. 8. |Real (δ)| versus ν for $s=5.237\times10^{-2}$, $\lambda_0 s=-0.13$ and $\varepsilon_0 s=0.39$

It is clearly shown in Fig. 8, that the difference $(\beta_l-\beta_t)$ is so large in this case—i.e. the strong coupling case—that the gain curves are largely separated into two regions. It is interesting to compare the values of β_t and β_l respectively with the values of $(\beta_e=\omega/v_0)_{\nu>0}$ and $(\beta_e=\omega/v_0)_{\nu<0}$ in which both are obtained from two values of ν—one is plus and the other minus—producing the maximum gains respectively, where,

$$\left.\begin{aligned} &\beta_t=1.29\,\beta_a\,, && \beta_l=0.58\,\beta_a \\ &(\beta_e)_{\nu>0}=1.29\,\beta_a\,, && (\beta_e)_{\nu<0}=0.54\,\beta_a \end{aligned}\right\} \qquad (37)$$

From the above results, it may be assumed that the discussion in the previous Section is reasonable (refer to Fig. 3). Though the difference $(\beta_l-(\beta_e)_{\nu<0})$ is somewhat large, it is due probably to larger error entering in the numerical gain calculations of ν on the minus case than in that of the plus case.

It is also seen from Fig. 8 that the maximum gain in the case of coupling with the slow wave, or β_t-wave is larger than that with the fast wave, or β_l-wave, but in respect to the range of ν producing the growing wave the former case is more narrow than the latter. Therefore if the high efficiency operation is desirable, it is better to utilize the faster wave. While the favourable view point of using the slow wave is based on the fact that the electron beam velocity

can be slowed down to such an extent as 75% velocity down when compared with the case of using β_a-wave. But, when there is no profit on slowing down the electron velocity, the circuit dimensions may be enlarged relatively without changing the electron velocity, being desirable for the higher frequency operation.

The calculation for the initial loss is made by using Eq. (27) and (29). For simplicity, the calculations are made only for two points i.e. $\nu=4.5$ and -16 which are respectively center points of separated two curves. The final results are as follows;

$$20\log|A|=\begin{cases}-10.6\,db & \text{for} \quad \nu=4.5\\ -3.5\,db & \text{for} \quad \nu=-16\end{cases} \tag{38}$$

However, it must be remembered here that the results of the initial losses by using Eq. (27) are not true practically because the fast electron space-charge wave has been completely neglected from all the analyses up to the present Section. In spite of the ignorance of this wave, however, the calculations of losses must be useful when the degree of initial losses is compared with several coupling conditions.

An outline of rigorous analysis including the fast electron space-charge wave is to be introduced in the next Section.

VI. The Rigorous Analysis not Neglecting the Fast Electron Space-Charge Wave

When the fast electron space-charge wave can not be neglected, the coupling equations Eq. (12) becomes useless and the next equations should be introduced.

$$\left.\begin{aligned}&\left\{d/dz+j\beta_c(1+\Delta)\right\}a_1=C_{12}a_2\\&(d/dz+j\beta_c)a_2=C_{21}a_1+C_{32}{}^*a_3-C_{42}{}^*a_4\\&\left\{d/dz+j\beta_e(1+C\sqrt{4QC})\right\}a_3=C_{32}a_2\\&\left\{d/dz+j\beta_e(1-C\sqrt{4QC})\right\}a_4=C_{42}a_2\end{aligned}\right\} \tag{39}$$

where

$$C_{32}=-C_{42}\,,\quad C_{23}=C_{32}{}^*,\quad C_{12}=-C_{21}{}^* \tag{40}$$

The last equation in Eq. (39) indicates the coupling between the fast electron space-charge wave and the circuit wave (2). The solutions of Eq. (39) are of the form $\exp(-\Gamma z)$, and substituting this form into Eq. (39) the next determinantal equation about the eigen-value Γ can be obtained.

$$\begin{vmatrix} -\Gamma+j\beta_e(1+\Delta) & -C_{12} & 0 & 0 \\ C_{12}^* & -\Gamma+j\beta_e & -C_{32}^* & -C_{32}^* \\ 0 & -C_{32} & -\Gamma+j\beta_e(1+C\sqrt{4QC}) & 0 \\ 0 & C_{32} & 0 & -\Gamma+j\beta_e(1-C\sqrt{4QC}) \end{vmatrix} = 0 \qquad (41)$$

If rewritten by using Eq. (14), then

$$(j\delta)^4+c_1(j\delta)^3+c_2(j\delta)^2+c_3(j\delta)+c_4=0\,, \qquad C\neq 0 \qquad (42)$$

where

$$\left.\begin{aligned} c_1 &= -(2b+|C_{12}'|^2+\lambda|C_{23}'|) \\ c_2 &= (|C_{12}'|^2+b)(\lambda|C_{23}'|+b)-4QC \\ c_3 &= 4QC(2b+|C_{12}'|^2+\lambda|C_{23}'|+1/2) \\ c_4 &= -4QC\left\{|C_{12}'|^2+(|C_{12}'|^2+b)(\lambda|C_{23}'|+b)\right\}-(b+\lambda|C_{23}'|)/2 \end{aligned}\right\} \qquad (43)$$

Now changing $j\delta$ to another form,

$$j\delta = x-c_1/4 \qquad (44)$$

then Eq. (42) can be rewritten as follows

$$x^4+px^2+qx+r=0 \qquad (45)$$

where

$$\left.\begin{aligned} p &= -(3/8)c_1^3+c_2 \\ q &= (1/8)c_1^3-(1/2)c_1c_2+c_3 \\ r &= -(3/256)c_1^4+(1/16)c_1^2c_2-(1/4)c_1c_3+c_4 \end{aligned}\right\} \qquad (46)$$

Now the next consideration is made for the following cubic equation.

$$z^3-pz^2-4rz+(4pr-q^2)=0 \qquad (47)$$

Assuming that z_1 is one of the three roots of Eq. (47), then four roots $x_i\,(i=1, 2, 3, 4)$ of Eq. (45) can be obtained from solving the next two quadratic equations

$$\left.\begin{aligned} &x^2+z_1/2=\sqrt{z_1-p}\,(x-q/2(z_1-p)) \\ \text{and}\quad &x^2+z_1/2=-\sqrt{z_1-p}\,(x-q/2(z_1-p)) \end{aligned}\right\} \qquad (48)$$

and $\delta_i(i=1, 2, 3, 4)$ are

$$j\delta_i = x_i-c_1/4\,, \qquad i=1, 2, 3, 4 \qquad (49)$$

When two of the roots δ_i are complex numbers, the exponential growing wave should exist. (It may be difficult to consider that the roots δ_i are all complex

numbers, because two different exponential growing waves may not exist simultaneously in this tube).

In fact, solving Eq. (42) to (49) is high elaborate, therefore, instead of solving those equations by hand, it would be convenient and more accurate to solve the values of δ by using electronic computer, if possible.

VII. Conclusion

It is concluded from the view-point of using no attenuator in the interaction space and of having the wide range of the electron beam velocity in which the growing wave can be produced, that this new type of tube is suitable for large-signal operations. Especially the case of the weak coupling strength at the coupled wall is more interesting than the case of the strong coupling strength, in comparing the following aspects on; (1) the suppresion of the reflex wave, (2) the range of the electron beam velocity in which the growing wave can be produced, (3) the difficulty in manufacturing, (4) and so forth.

This paper is somewhat insufficient to design actually this new type of tube, but this will be defered to next chance.

Acknowledgment

The author wishes to thank the staff of the department of electronic engineering, Hokkaido University, for their suggestions and constructive criticisms.

References

1) William H. Louisell: "Coupled Mode and Parametric Electronics". John Wiley & Sons, Inc., Publishers.
2) S. Saito: "Denshi-beam Denzi Kairo Ron". OHM Shya.
3) J. R. Pierce: "Traveling-Wave Tubes". D. Van Nostrand Company, Inc., 1950.
4) J. S. Cook, R. Kompfner and C. F. Quate: "Coupled Helices". The Bell System Technical Journal, January 1956.